CONFIDENTIAL

RM SE9J14

NACA

RESEARCH MEMORANDUM

for the

Air Materiel Command, U. S. Air Force

PERFORMANCE OF AXIAL-FLOW SUPERSONIC COMPRESSOR

OF THE XJ55-FF-1 TURBOJET ENGINE

IV - ANALYSIS OF COMPRESSOR OPERATION

OVER A RANGE OF EQUIVALENT TIP SPEEDS

FROM 801 TO 1614 FEET PER SECOND

By Robert C. Graham and Melvin J. Hartmann

Lewis Flight Propulsion Laboratory
Cleveland, Ohio

NATIONAL ADVISORY COMMITTEE
FOR AERONAUTICS
WASHINGTON

NOVEMBER 18 1949

CONFIDENTIAL

CLASSIFICATION CANCELLED

CONFIDENTIAL

NATIONAL ADVISORY COMMITTEE FOR AERONAUTICS

RESEARCH MEMORANDUM

for the

Air Materiel Command, U.S. Air Force

PERFORMANCE OF AXIAL-FLOW SUPERSONIC COMPRESSOR

OF THE XJ55-FF-1 TURBOJET ENGINE

IV - ANALYSIS OF COMPRESSOR OPERATION

OVER A RANGE OF EQUIVALENT TIP SPEEDS

FROM 801 TO 1614 FEET PER SECOND

By Robert C. Graham and Melvin J. Hartmann

SUMMARY

An investigation was conducted to determine the performance characteristics of the axial-flow supersonic compressor of the XJ55-FF-1 turbojet engine. An analysis of the performance of the rotor was made based on detailed flow measurements behind the rotor.

The compressor apparently did not obtain the design normal-shock configuration in this investigation. A large redistribution of mass occurred toward the root of the rotor over the entire speed range; this condition was so acute at design speed that the tip sections were completely inoperative. The passage pressure recovery at maximum pressure ratio at 1614 feet per second varied from a maximum of 0.81 near the root to 0.53 near the tip, which indicated very poor efficiency of the flow process through the rotor. The results, however, indicated that the desired supersonic operation may be obtained by decreasing the effective contraction ratio of the rotor blade passage.

INTRODUCTION

At the request of the Air Materiel Command, U.S. Air Force, the NACA Lewis laboratory is conducting an investigation of the

performance characteristics of the axial-flow supersonic compressor
of the XJ55-FF-1 turbojet engine. The compressor installation
consists of a row of inlet guide vanes and a supersonic rotor
(fig. 1). The performance of the inlet guide vanes as a separate
component is presented in reference 1 and the over-all performance
of the compressor is presented in references 2 and 3. Reference 3
indicates that the design-shock configuration was not obtained, but
does not suggest possible reasons for this departure from design
operation.

An analysis based on a radial survey 3/4 inch downstream of the
trailing edge of the rotor was therefore made in order to obtain
some insight into the flow processes in the rotor and to provide a
means of determining the reasons for the divergence from design
performance. The results of the analysis of these survey data and
calculated entrance conditions are presented herein as well as sug-
gested methods for improving the compressor performance.

During the present investigation, damage was incurred to the
leading edges of the rotor blades (described in reference 3), which
necessitated refinishing the blades. Data presented herein were
obtained both before the damage and after the first reworking of
the blades and, as pointed out in reference 3, are a reliable
representation of the undamaged compressor.

The instrumentation, the apparatus, and the general test pro-
cedure used in this investigation are described in reference 3.
A schematic drawing of the compressor installation is shown in
figure 2.

SYMBOLS

The following symbols are used in this report:

C_r contraction ratio, ratio of entrance to minimum area where
        entrance area is taken as area from leading edge of one
        blade to surface of next blade normal to flow path

M absolute Mach number, ratio of absolute air velocity to
        local velocity of sound

M' relative Mach number, ratio of air velocity relative to
        rotor to local velocity of sound

n rotor speed, (rps)

P total or stagnation pressure, (lb/sq ft)

P' total or stagnation pressure of air relative to rotor, (lb/sq ft)

p static or stream pressure, (lb/sq ft)

r compressor radius, (ft)

T total or stagnation temperature, ($^{\circ}$R)

t static or stream temperature, ($^{\circ}$R)

U velocity of rotor at radius r, $2\pi rn$, (ft/sec)

W weight flow, (lb/sec)

α angle between compressor axis and trailing blade surface at leading edge, (deg)

β angle between compressor axis and absolute air direction (deg)

β' angle between compressor axis and air direction relative to rotor, (deg)

γ ratio of specific heats for normal air, 1.40

δ ratio of actual inlet pressure to standard sea-level pressure, $P_1/2116$

η_{ad} adiabatic efficiency, $\dfrac{T_1\left[(P_5/P_1)^{\frac{\gamma-1}{\gamma}} - 1.0\right]}{T_5 - T_1}$

θ ratio of actual inlet stagnation temperature to standard sea-level temperature, $T_1/518.4$

φ angle between compressor axis and the average between leading and trailing surfaces of blades at rotor exit, (deg)

Subscripts:

1 compressor entrance (depression tank)

2 rotor entrance

5   rotor exit

t   tip

z   axial component

θ   tangential component

PROCEDURE

The analysis of the flow processes in the rotor was based on a detailed radial survey 3/4 inch downstream of the rotor and on calculated radial distribution at the rotor entrance.

Rotor-entrance conditions were calculated on the basis of static-pressure readings of wall taps located on the inner and outer housing immediately upstream of the rotor leading edge. A linear variation in static pressure was assumed between root and tip. The total pressure as measured at the compressor inlet, less an assumed 1-percent loss through the guide vanes (reference 1), was used in the calculations. Because there was only a 1° variation in the guide-vane turning angle with Mach number (reference 1), average turning angles were used in calculating entrance conditions relative to the rotor.

Absolute and relative velocities and angles at the rotor exit were calculated from the direct measurement of total pressure P_5, static pressure p_5, flow angle β_5, rotational velocity U, and total temperature T_5. The general relations used to calculate entrance and exit conditions are:

$$\frac{P}{p} = \left(1 + \frac{\gamma-1}{2} M^2\right)^{\frac{\gamma}{\gamma-1}}$$

$$\frac{T}{t} = 1 + \frac{\gamma-1}{2} M^2$$

RESULTS

Over-All Performance

The over-all performance characteristics of the supersonic compressor of the XJ55-FF-1 engine are shown in figure 3. These data are presented and discussed in detail in reference 3.

Performance at Maximum Pressure Ratio at Design Speed

The entrance conditions relative to the rotor at maximum pressure ratio at an equivalent tip speed of 1614 feet per second are shown in figure 4. The distribution of relative entrance-air angle β'_2 and relative entrance Mach number M'_2 across the annulus is shown as calculated from wall static-pressure readings. The relative entrance Mach number is 15 percent lower than design at the root and 7 percent lower at the tip (fig. 4(a)). This low entrance Mach number results in an appreciable positive angle of attack, ranging, from 6° to 7° across the blade span, as shown by the difference between the relative air angle β'_2 and blade angle α (fig. 4(b)). (Angle of attack is defined as the difference between the relative entrance air angle β'_2 and the blade angle α shown in fig. 5.) The design provides a 3° positive angle of attack at the root and a 3° negative angle of attack at the tip (reference 4). It is apparent that this design standing-wave pattern was not obtained, as the calculated entrance conditions indicate that a 6° to 7° positive angle of attack existed along the entire span.

The maximum compressor total-pressure ratio P_5/P_1, obtained at an equivalent tip speed of 1614 feet per second, is plotted as a function of radius in figure 6. This curve shows that the highest pressure ratio is obtained near the root and falls off sharply toward the tip.

The axial component of the measured exit and calculated entrance Mach number is shown in figure 7. Measured axial exit velocity varies considerably from root to tip, actually diminishing to zero at the tip; this distribution shows a considerable variation from the design. Comparison of the entrance and exit curves indicates a large redistribution of mass flow toward the root of the blades. The axial velocity at the outlet of the guide vanes, presented in reference 1, is not in complete agreement with the calculated axial velocity (fig. 7), but considering the axial velocities from reference 1, an even larger redistribution through the rotor would be indicated.

A plot of relative exit Mach number and relative exit-air angles
for an equivalent tip speed of 1614 feet per second is shown in fig-
ure 8, along with the design relative exit Mach number and mean blade
angle. Figure 8 shows extremely high Mach numbers near the root,
decreasing toward the tip, and relative exit-air angles reaching 90°
at the tip. With the absolute exit-air angles near 90°, the air at
the tip will travel a considerable distance around the outer hous-
ing before reaching the survey instrument; thus friction will reduce
the absolute velocity well below the rotation speed of the wheel.
The resultant relative exit velocity is therefore large, with an
axial velocity near zero and a relative exit-air angle approach-
ing 90°.

The passage pressure recovery P'_5/P'_2 is plotted as a function
of total weight flow in figure 9. The pressure recovery in effect
represents the flow efficiency between stations 2 and 5. Due to the
large exit-air angles, the air may travel several inches between the
rotor exit and the survey instrument downstream of the wheel; the
recovery presented therefore contains losses other than those incurred
in the rotor passage. Figure 9 shows that the recovery varies from
approximately 80 percent near the root to 55 percent near the tip,
and provides evidence of a very inefficient flow process.

Performance at Maximum Pressure Ratio over Range of Tip Speeds

Entrance conditions relative to the rotor at maximum pressure
ratio and equivalent tip speeds of 801, 1204, and 1614 feet per sec-
ond are shown in figure 10. The relative entrance-air angle, blade
angle, and the subsequent positive angle of attack are shown in this
figure. The angle of attack decreases $1/2^\circ$ at the root to 1° at the
tip as the equivalent tip speed is increased from 801 to 1614 feet
per second. Relative exit Mach number plotted as a function of the
radius for equivalent tip speeds of 801, 1204, and 1614 feet per
second are shown in figure 11. The exit Mach number falls off from
root to tip throughout the speed range, resulting in a distribution
that departs appreciably from design. The distribution of exit
Mach number remains essentially the same over the speed range.

The relative exit-air angle β'_5 is plotted as a function of
radius for equivalent tip speeds of 801, 1204, and 1614 feet per
second in figure 12. As the speed increases the exit-air angle
increases at any given radius. At 801 feet per second, the relative
air angle closely approximates the mean blade angle φ (fig. 5) from
the root to the pitch radius, but diverges sharply from the pitch
radius to the tip. As the speed is increased, the air angle at the

root increases and the point at which the slope of the curve breaks
away from the mean blade angle is closer to the root. Relative exit-
air angles at the tip are excessive at all speeds. This extreme dis-
tribution would create a considerable problem of recovering the energy
in the stator blades.

Performance at 1396 Feet Per Second over Range of Pressure Ratios

The entrance conditions relative to the rotor, plotted as a
function of radius for various pressure ratios at an equivalent tip
speed of 1396 feet per second, are shown in figure 13. From these
curves it can be seen that the entrance conditions do not change
materially over the range of pressure ratios investigated. The angle
of attack and the entrance Mach number remain essentially constant
with pressure ratio at this speed and there is an insignificant vari-
ation of angle of attack with radius. The relative entrance Mach
number also remains essentially constant from root to tip.

Total-pressure ratio, relative exit Mach number, and relative
exit-air angle are plotted as functions of radius for a range of
pressure ratios in figures 14, 15, and 16, respectively. The trend
of falling pressure ratio from root to tip is prevalent at all pres-
sure ratios; however, the radial distribution does improve with
increasing pressure ratio.

Increasing pressure ratio has no apparent effect on the relative
exit Mach number distribution. The Mach numbers are high near the
root, decreasing sharply toward the tip; and relative exit-angle dis-
tribution remains essentially constant over the pressure-ratio range.
Excessively high angles were experienced at the tip at all pressure
ratios.

DISCUSSION

Theoretical operation. - At low speeds where the relative inlet
velocity is subsonic, the theoretical operation of this type of
compressor is comparable to that of the subsonic axial-flow
compressor. At relative entrance Mach numbers slightly over 1.0, a
detached bow wave is formed, which becomes stronger and more nearly
attached to the leading edges of the blades as the speed is increased.
Finally, when the design supersonic operation is reached, the bow
waves become attached, and the passage-contained normal-shock con-
figuration is established.

If the compressor does not attain design supersonic operation, that is, a rotor-contained normal shock, poor efficiency of the flow process would be expected. It is likely that if the compressor fails to attain this condition of supersonic operation, hereinafter referred to as "starting", the resultant shock configuration will be in the form of a strong detached bow wave. With such a shock configuration, the efficiency would be expected to fall off as the speed is increased through the supersonic range, rather than remaining essentially constant. The failure of the compressor to start is evident from the restriction of the flow (reference 3).

With a variable back pressure, the failure of a compressor of this type to start can generally be attributed to one or more of the following reasons:

(1) Too large a wedge angle; that is, too large an angle between driving and trailing surfaces at the leading edge

(2) Too high a contraction ratio C_r for the relative entrance Mach number

(3) Boundary-layer build-up along the inner and outer shrouds and on the blade surface, which effectively reduces the minimum area

Boundary-layer growth would cause the effective contraction ratio to be substantially larger than the geometric contraction ratio.

Actual operation. - Examination of the data indicates that this compressor did not attain design supersonic operation at an equivalent tip speed of 1614 feet per second. A continual decrease in efficiency with increasing speed (fig. 3), along with the exceedingly poor efficiency attained at high speed, offer strong indication of the failure of the compressor to obtain the design-shock configuration. Further indication of the failure of this compressor to start is the equivalent weight flow measured at 1614 feet per second, which was 17.5 percent below design. In the supersonic-compressor investigation described in reference 5, angles of attack were from 6° to 10°, decreasing to 2° when supersonic operation was attained. A comparison of the angles of attack obtained in this investigation with those presented in reference 5 further indicates that supersonic operation was not reached.

The wedge angles used in this design are sufficienctly small to allow starting at the design Mach number. The geometric contraction ratio is small enough to allow the compressor to start. It seems probable, however, that the boundary-layer build-up along the shrouds

and the blades would be sufficient to create an effective con-
traction ratio too large to allow starting at the design relative
entrance Mach number. It is therefore probable that the primary
cause of the poor performance of the compressor investigated is too
high an effective contraction ratio.

As previously shown, at design speed the concentration of
mass and the greater pressure rise produced at the root, along with
the extremely low pressure recovery at the tip, indicate clearly
that the greater portion of useful work is being done near the hub
of the compressor. The air at the tip is essentially rotating with
the blades, having only a small component of axial velocity; thus
the tip sections are essentially inoperative. As pointed out in
reference 5, in order to obtain satisfactory performance of the
supersonic compressor operating at nearly maximum contraction ratio,
the entire passage must be effective; a relatively small reduction
in effective passage area results in a large reduction in
performance.

Several possible explanations exist for the concentration of
low-momentum air at the tip. It is probable that one of the pri-
mary causes is an excessive boundary-layer collection along the
outer shroud. The pressure gradient over the rotor is such that
separation of the heavy boundary layer is likely. Another possible
explanation is the centrifuging of the separated boundary layer
from the subsonic portion of the blade passage, because the design
subsonic diffusion rate is sufficiently large to make separation
probable.

Method of obtaining supersonic operation. - As previously
pointed out, the primary factor restricting the starting of the
supersonic compressor is the high effective contraction ratio.
In order to obtain supersonic operation of this compressor, the
effective contraction ratio must therefore be reduced. A sub-
stantial improvement in the performance would be expected if the
compressor could be made to start. It has been found that the
starting characteristics of the supersonic compressor are very
critical and only a small change in contraction ratio may be
required when operation is marginal.

One method of reducing the contraction on this compressor
would involve revision of the outer rotor housing. Modification
of the housing to provide a cylindrical surface would increase the
three-dimensional area at the minimum section, thus lowering the
passage contraction ratio.

A second method of effectively decreasing the contraction ratio would be removal of mass at the minimum section. Removal of the stagnant air by bleedoff through the stationary outer casing would increase the effective minimum area, thus aiding shock entry.

SUMMARY OF RESULTS

The following results were obtained from the analysis of results of the investigation of the supersonic compressor of the XJ55-FF-1 turbojet engine:
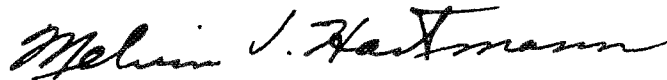
1. The compressor apparently did not attain supersonic operation at an equivalent tip speed of 1614 feet per second. The results, however, indicated that the desired operation may be obtained by decreasing the effective contraction ratio of the rotor blade passage.

2. A large redistribution of mass flow occurred toward the root of the rotor over the entire speed range. The condition was so acute at design speed that the passage near the tip was essentially inoperative.

3. Relative exit-air angles ranged from approximately 40° at the root to 90° at the tip at maximum pressure ratio and an equivalent tip speed of 1614 feet per second. This extreme distribution would create a considerable problem in the stator blades.

4. The passage pressure recovery at maximum pressure ratio
varied from a maximum of 0.81 at the root to 0.53 near the tip at
an equivalent tip speed of 1614 feet per second, which indicated a
very poor efficiency of the flow process.

Lewis Flight Propulsion Laboratory,
National Advisory Committee for Aeronautics,
Cleveland, Ohio, August 25, 1949.

Robert C. Graham,
Aeronautical Research Scientist.
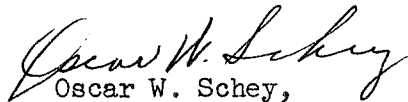
Melvin J. Hartmann,
Aeronautical Research Scientist.

Approved:
Robert O. Bullock,
Aeronautical Research Scientist.

Oscar W. Schey,
Aeronautical Research Scientist.

cag

REFERENCES

1. Graham, Robert C., and Tysl, Edward R.: Performance of Axial-
   Flow Supersonic Compressor of XJ55-FF-1 Turbojet Engine. II -
   Performance of Inlet Guide Vanes as Separate Component. NACA
   RM SE9E03, U.S. Air Force, 1949.

2. Hartmann, Melvin J., and Graham, Robert C.: Performance of
   Axial-Flow Supersonic Compressor of XJ-55-FF-1 Turbojet Engine.
   I - Preliminary Performance of Compressor. NACA RM SE9A31,
   U.S. Air Force, 1949.

3. Hartmann, Melvin J., and Tysl, Edward R.: Performance of Axial-
   Flow Supersonic Compressor of XJ55-FF-1 Turbojet Engine. III -
   Over-All Performance of Compressor. NACA RM SE9G19, U.S. Air
   Force, 1949.

4. Blanton, J., and Dunlavy, H.: Aerodynamic and Thermodynamic
   Design of the Compressor for the XJ-55-FF-1 Gas Turbine. Rep.
   No. 124-R4, Frederic Flader, Inc. (North Tonawanda, N. Y.),
   Sept. 25, 1947.

5. Johnsen, Irving A., Wright, Linwood C., and Hartmann, Melvin J.:
   Performance of 24-Inch Supersonic Axial-Flow Compressor in Air.
   II - Performance of Compressor Rotor At Equivalent Tip Speeds
   from 800 to 1765 Feet per Second. NACA RM E8G01, 1949.
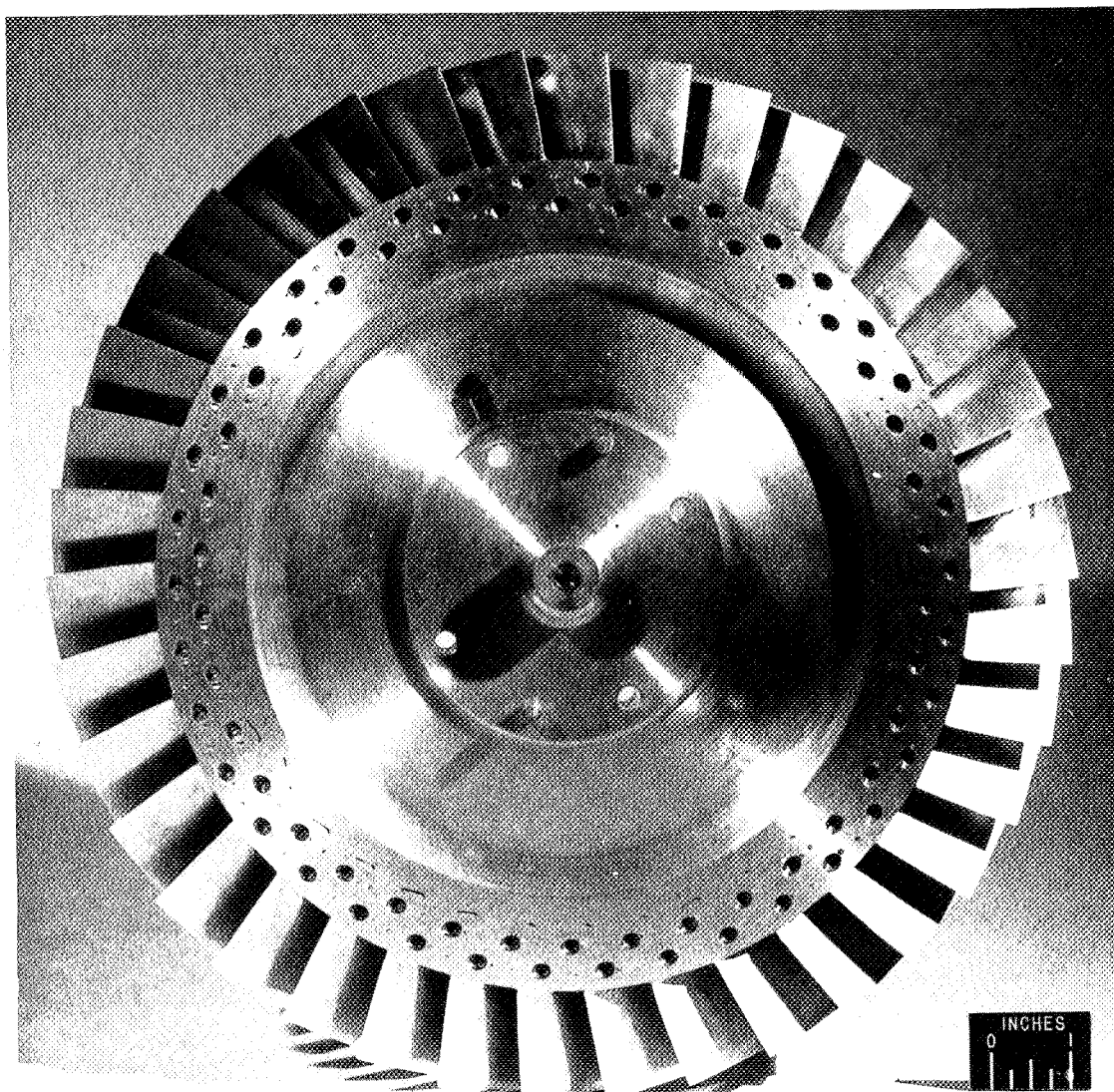
Figure 1. - Supersonic rotor of XJ55-FF-1 turbojet engine.
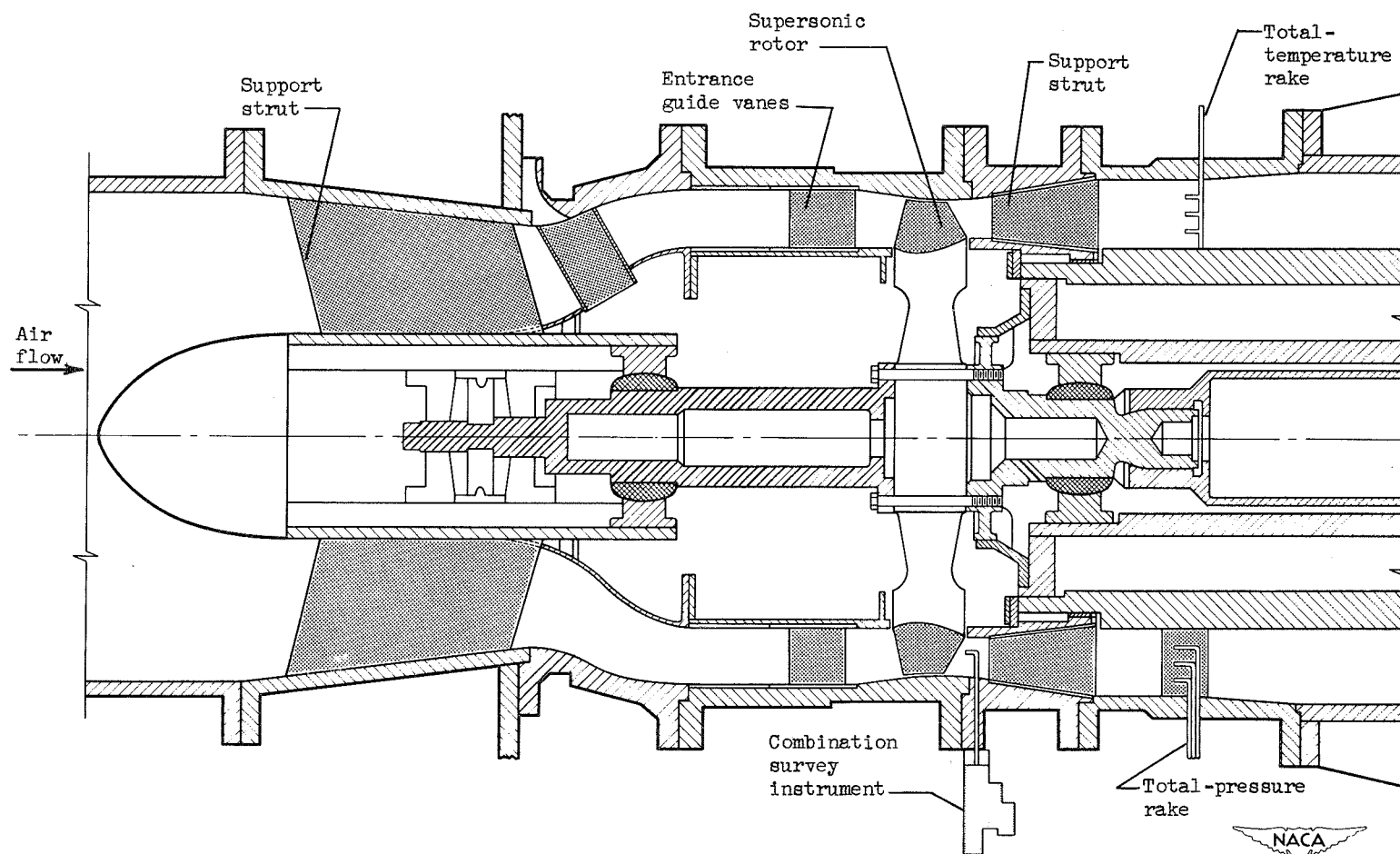
Figure 2. - Schematic drawing of XJ55-FF-1 supersonic-compressor installation.
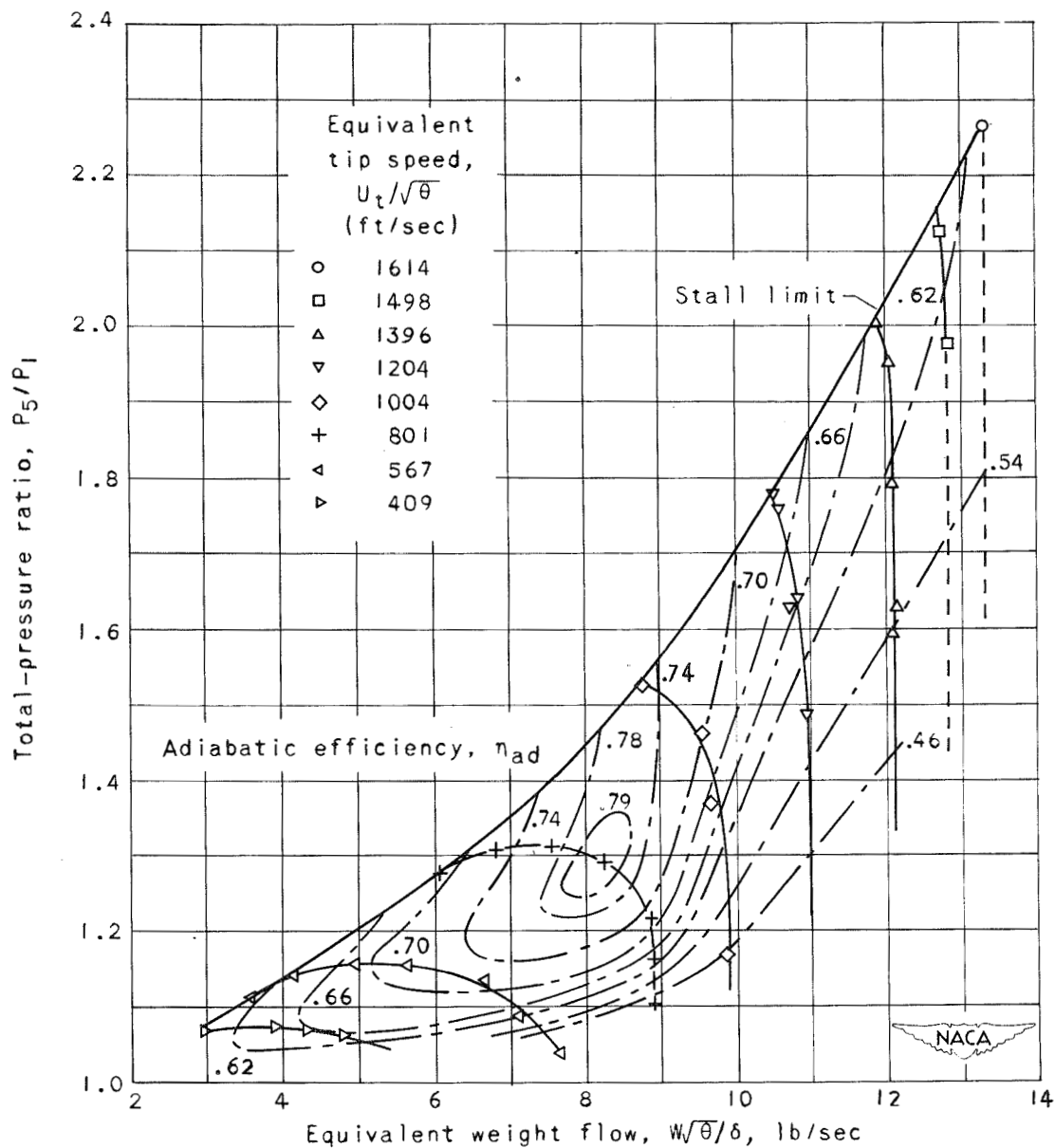
Figure 3. – Performance characteristics of axial-flow supersonic
compressor for XJ55–FF–1 turbojet engine. (Fig. 6 of
reference 2.)
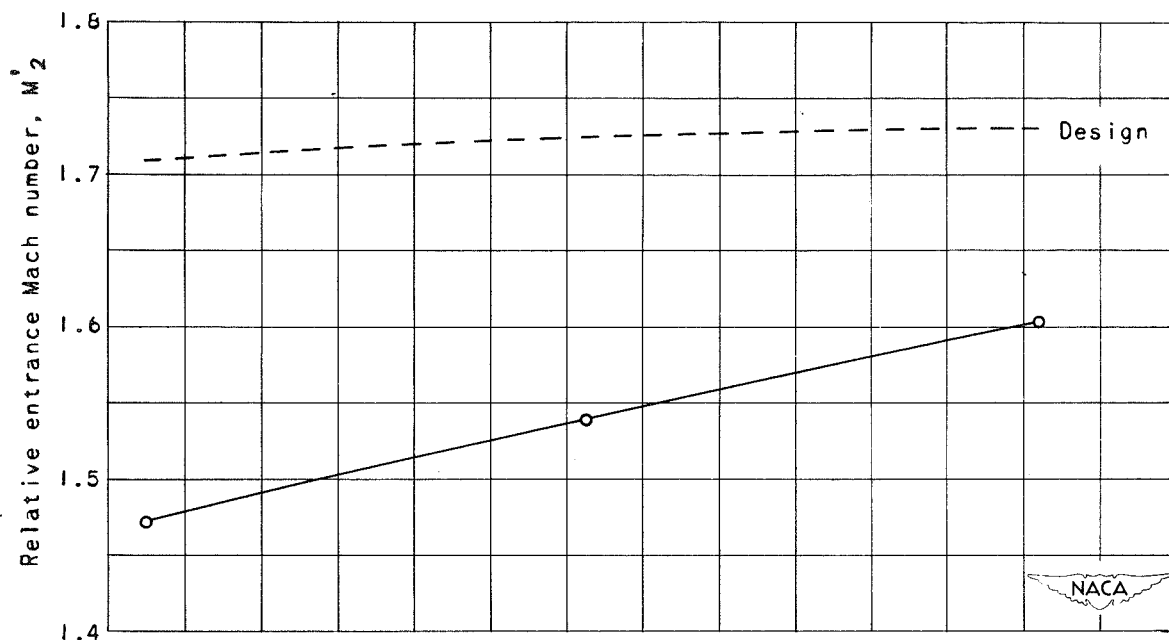
(a)   Relative entrance Mach number.
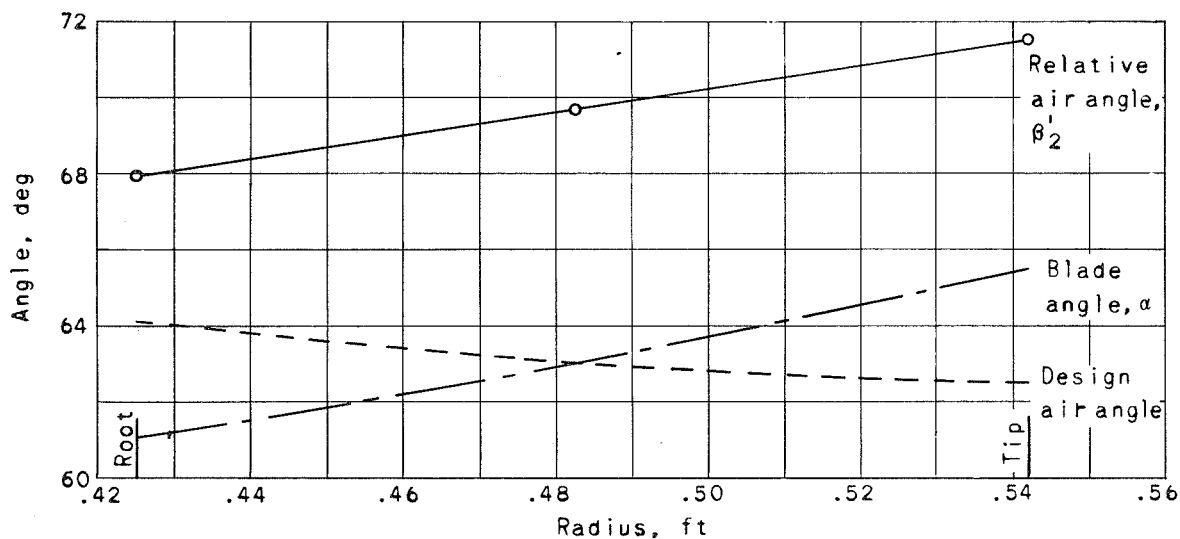
(b)   Relative air angle and blade angle.

Figure 4. — Entrance conditions relative to rotor at maximum pressure
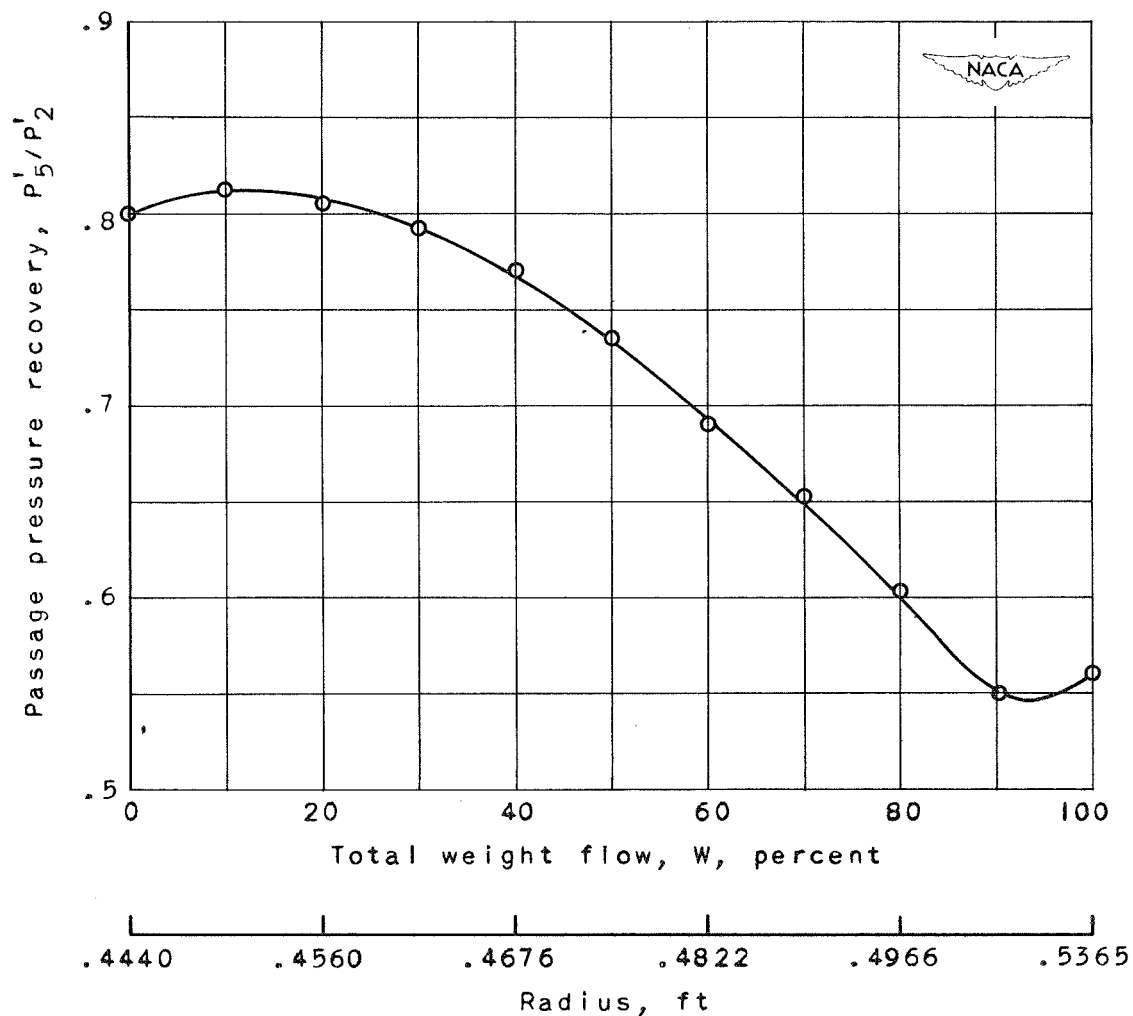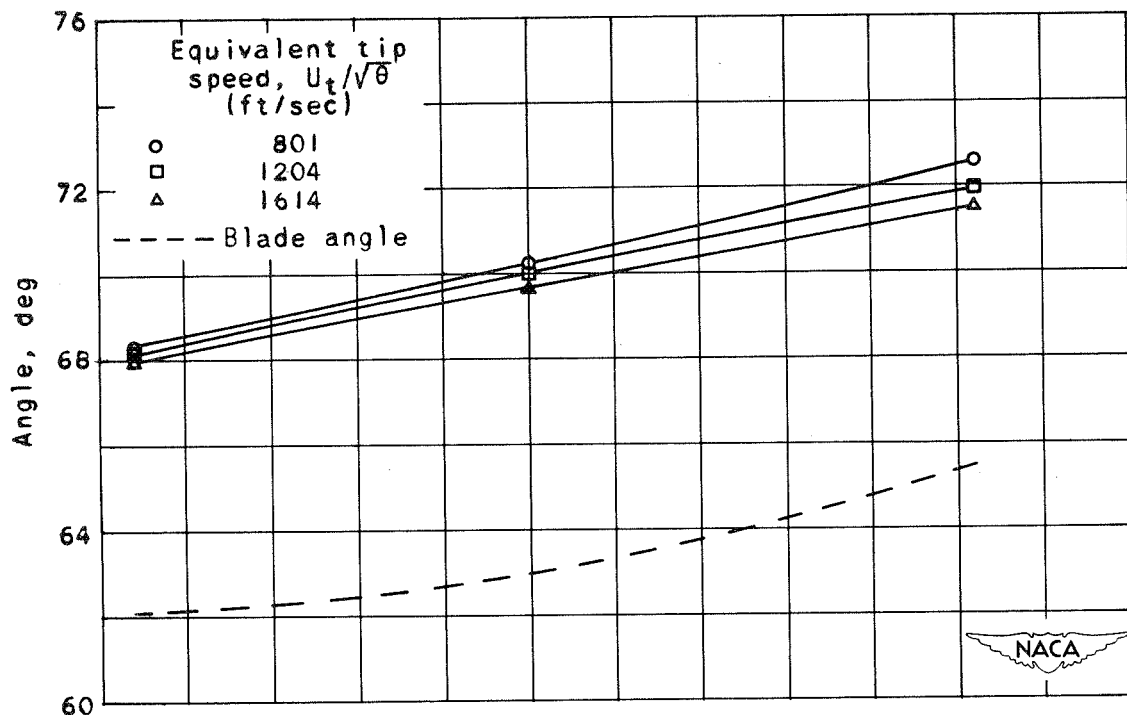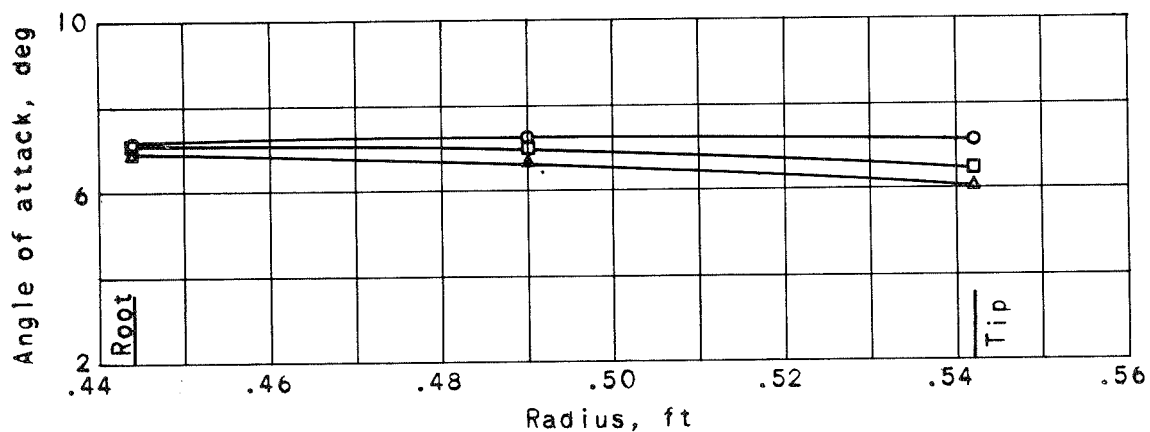ratio and equivalent tip speed of 1614 feet per second.
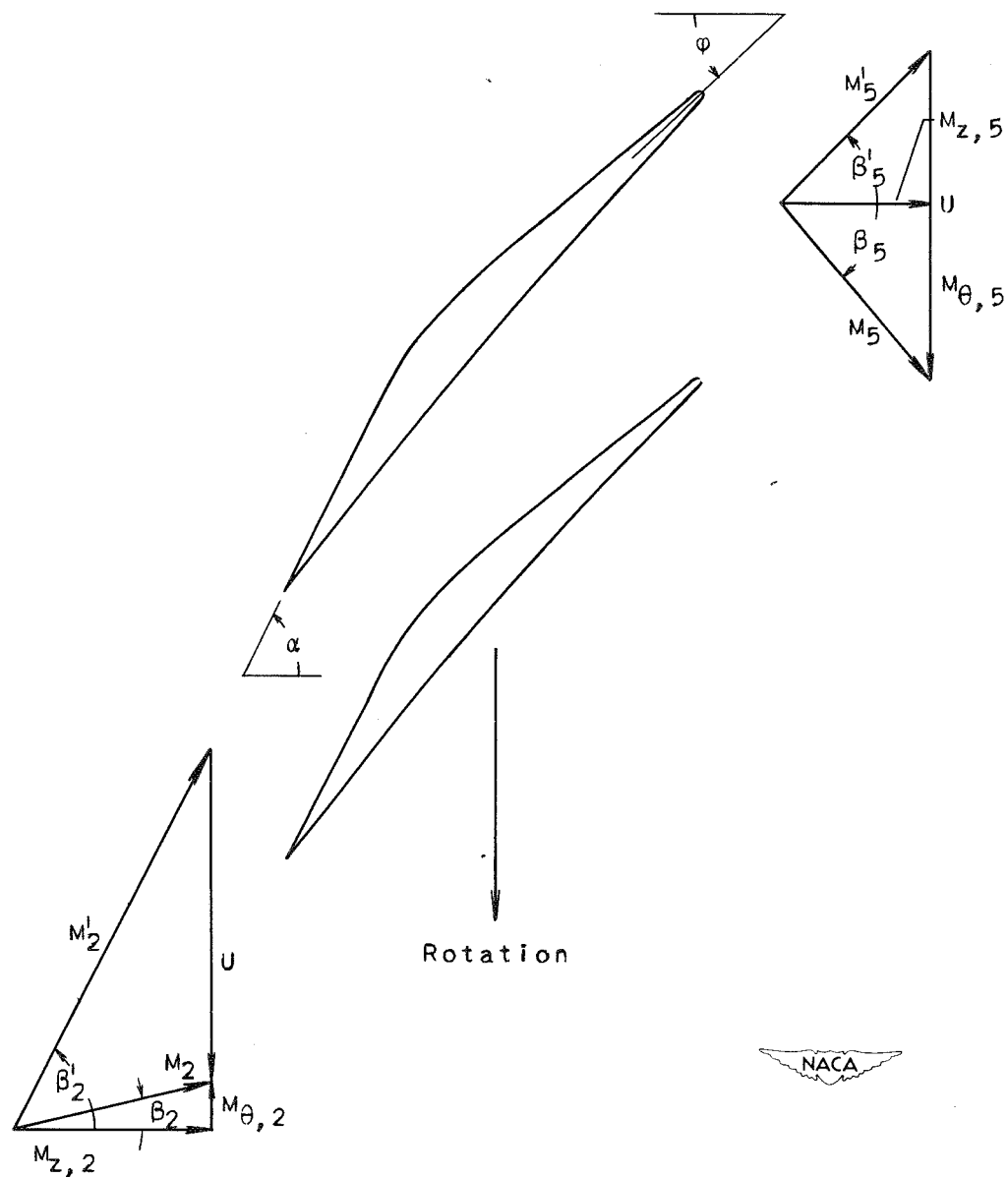
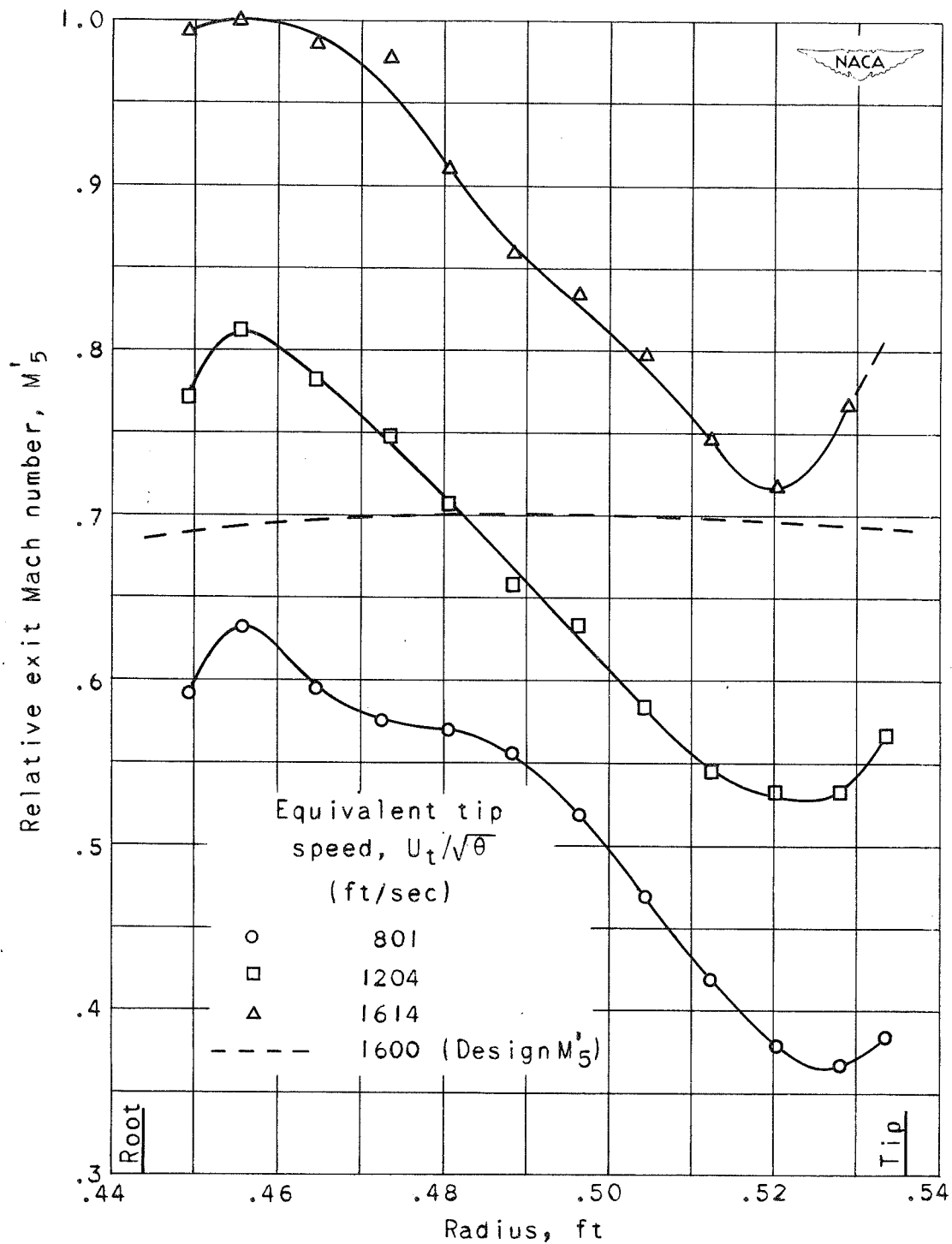Figure 5. — Typical velocity diagram.
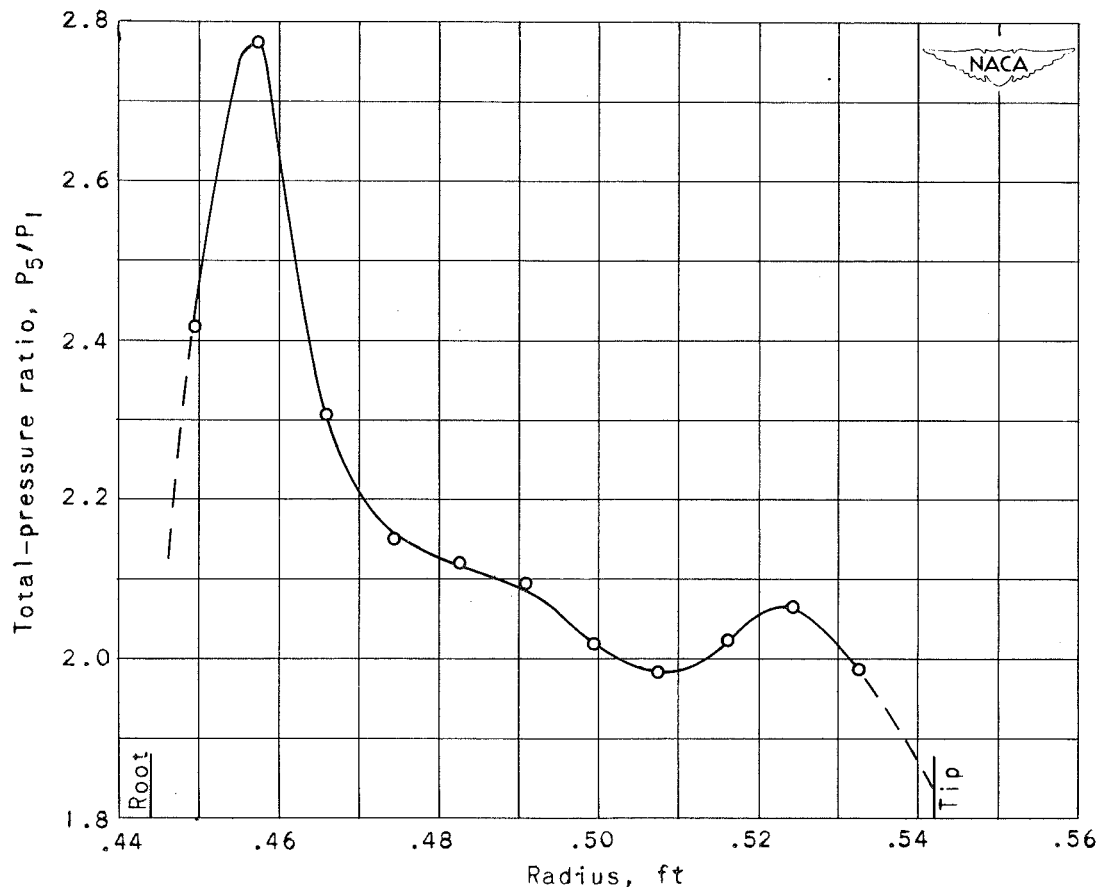
Figure 6. — Variation of total—pressure ratio with radius at maximum pressure ratio and equivalent tip speed of 1614 feet per second.
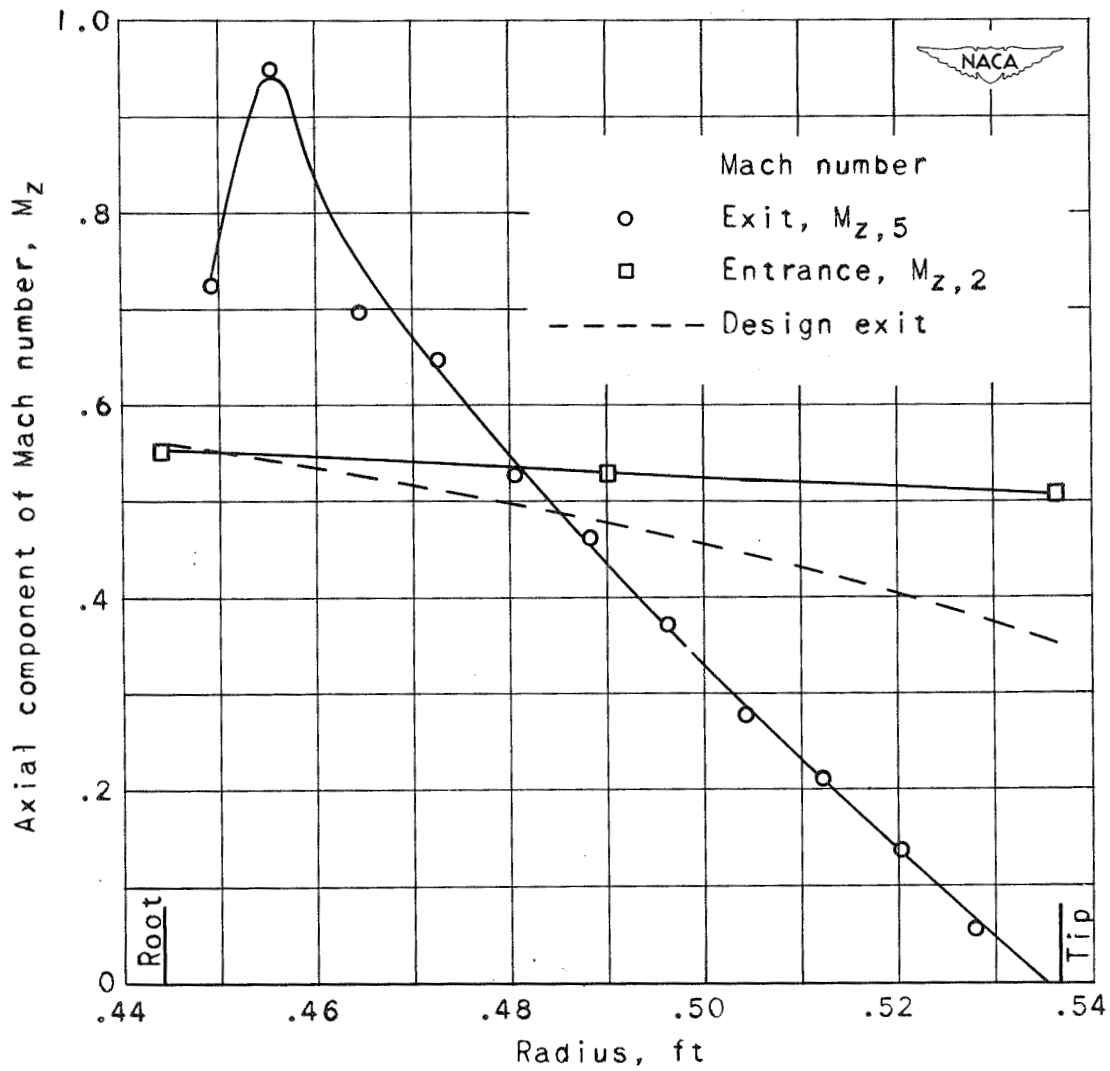
Figure 7. — Axial component of entrance and exit Mach number at maximum pressure ratio and equivalent tip speed of 1614 feet per second.
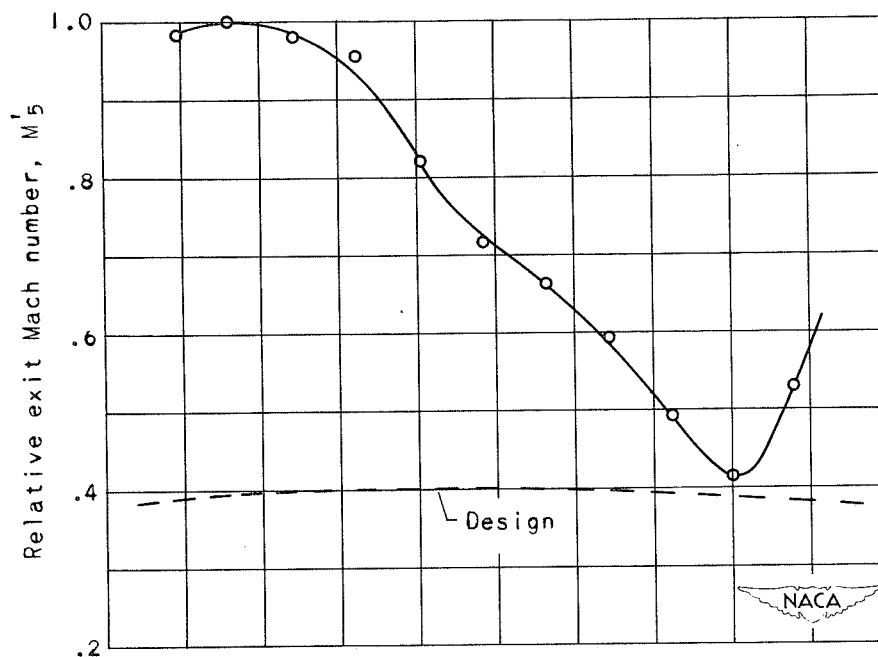
(a) Relative exit Mach number.
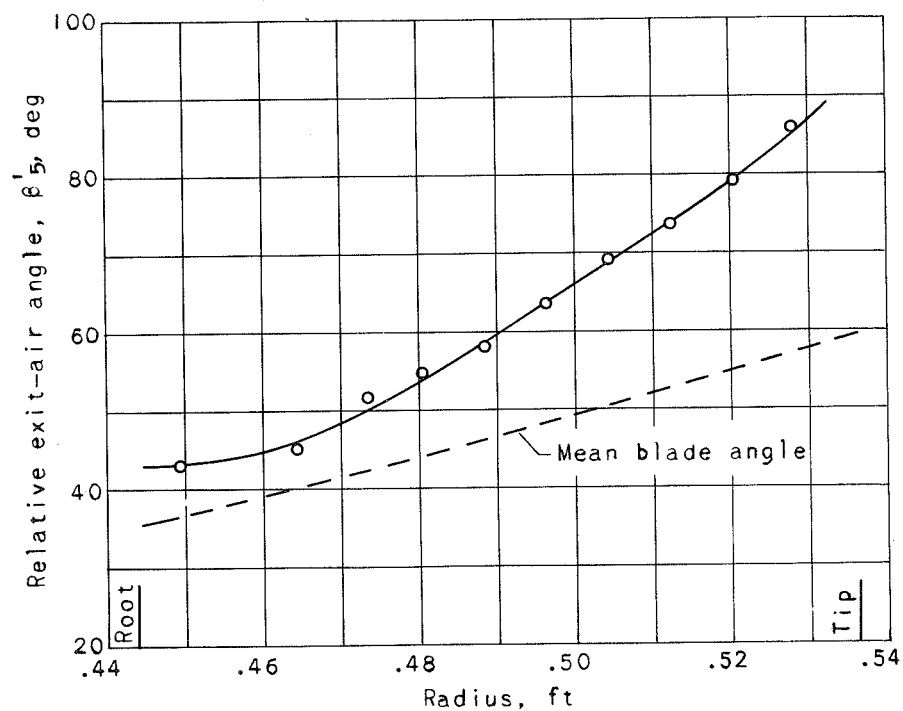
(b) Relative exit-air angle.

Figure 8. – Exit conditions relative to rotor at
maximum pressure ratio and equivalent tip speed of
1614 feet per second.

Figure 9. — Passage pressure recovery at maximum
    pressure ratio and equivalent tip speed of 1614 feet
    per second.

(a)   Relative entrance-air angle and blade angle.

(b)   Angle of attack.

Figure 10. - Entrance conditions relative to rotor at maximum
pressure ratio and several equivalent tip speeds.

Figure II. — Variation of relative exit Mach number with radius at maximum pressure ratio and several equivalent tip speeds.
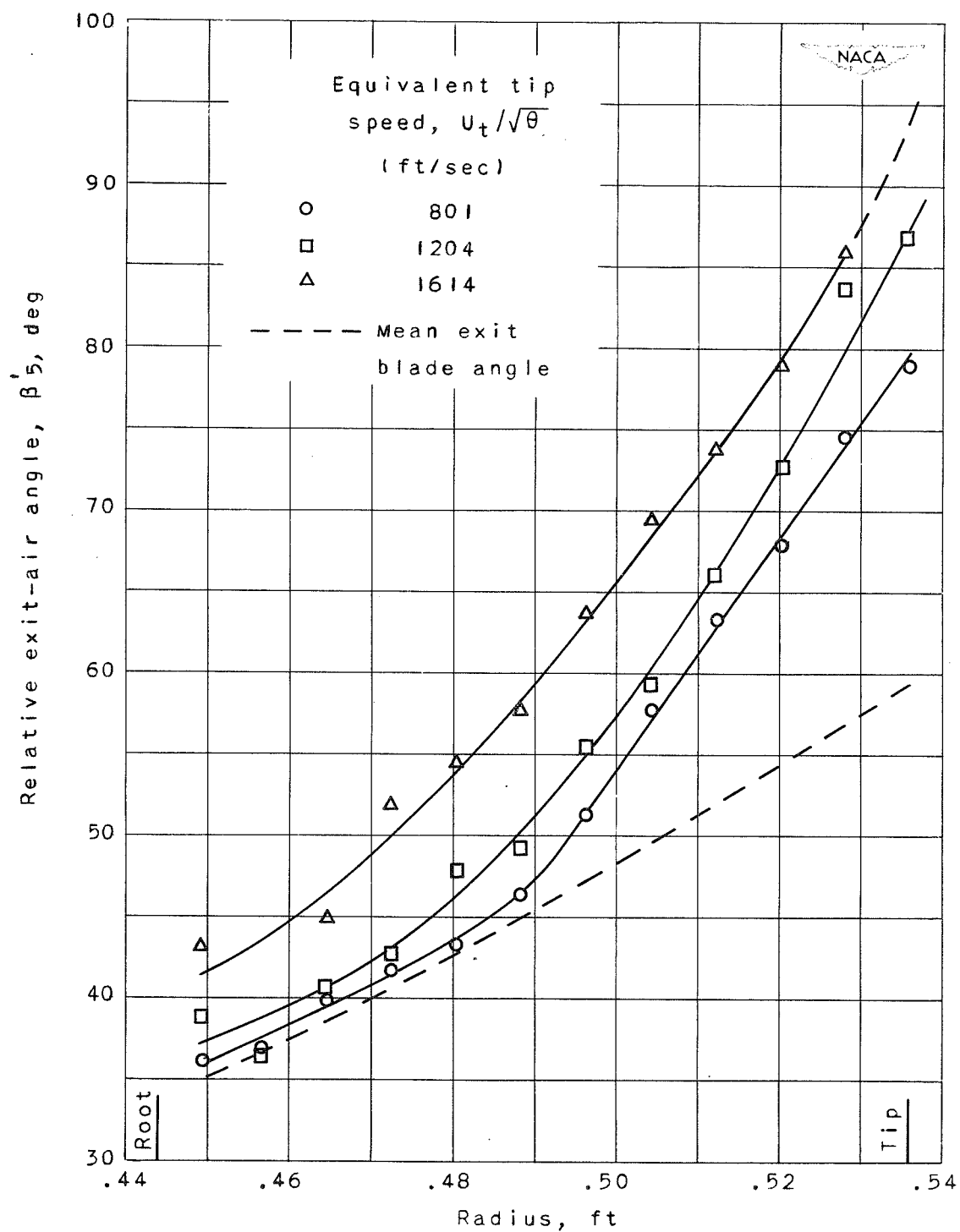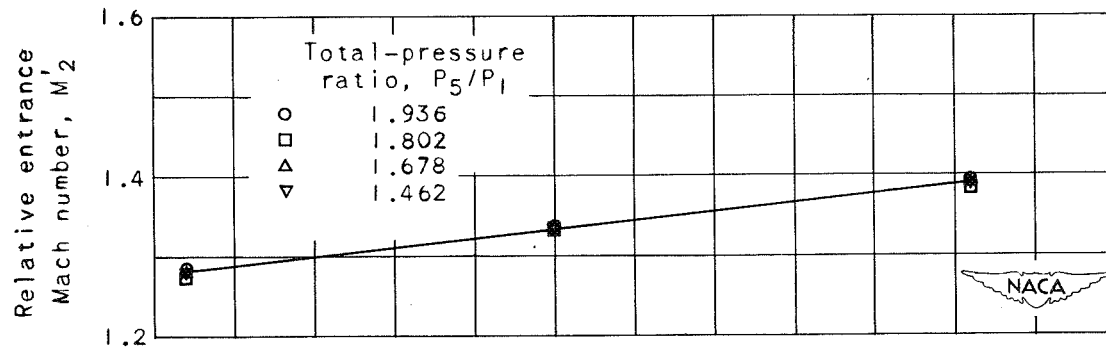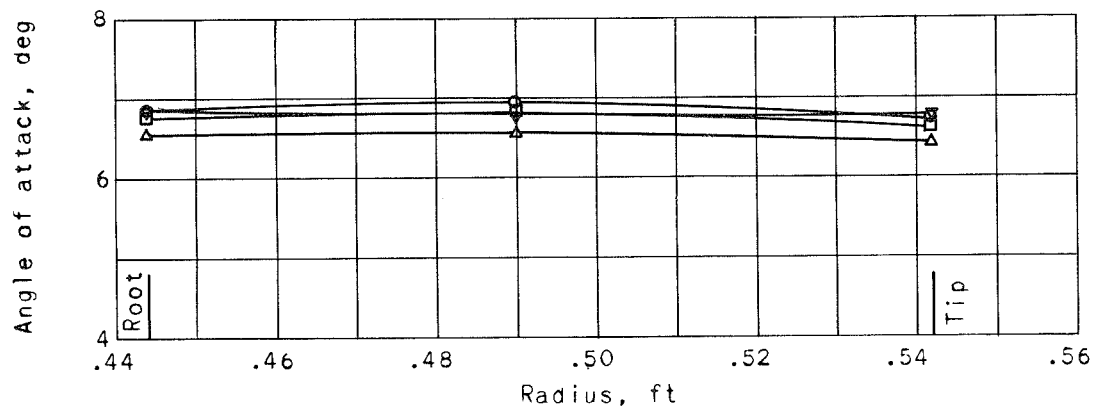
Figure 12. — Variation of relative exit—air angle with radius at maximum pressure ratio and several equivalent tip speeds.

(a)   Relative entrance Mach number.

(b)   Angle of attack.

Figure 13. — Entrance conditions relative to rotor at equivalent
    tip speed of 1396 feet per second for various pressure
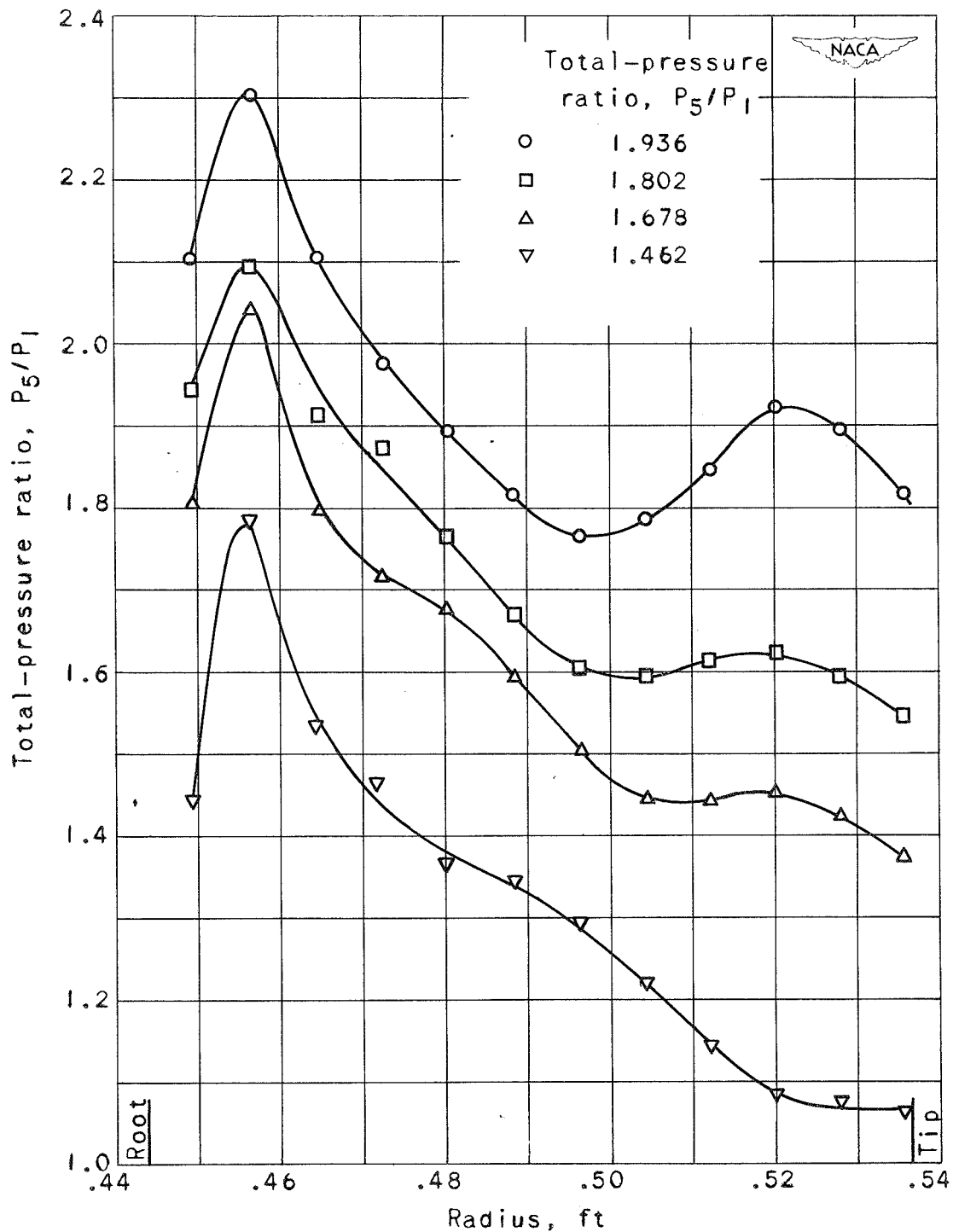   ratios.

Figure 14. — Variation of total-pressure ratio with
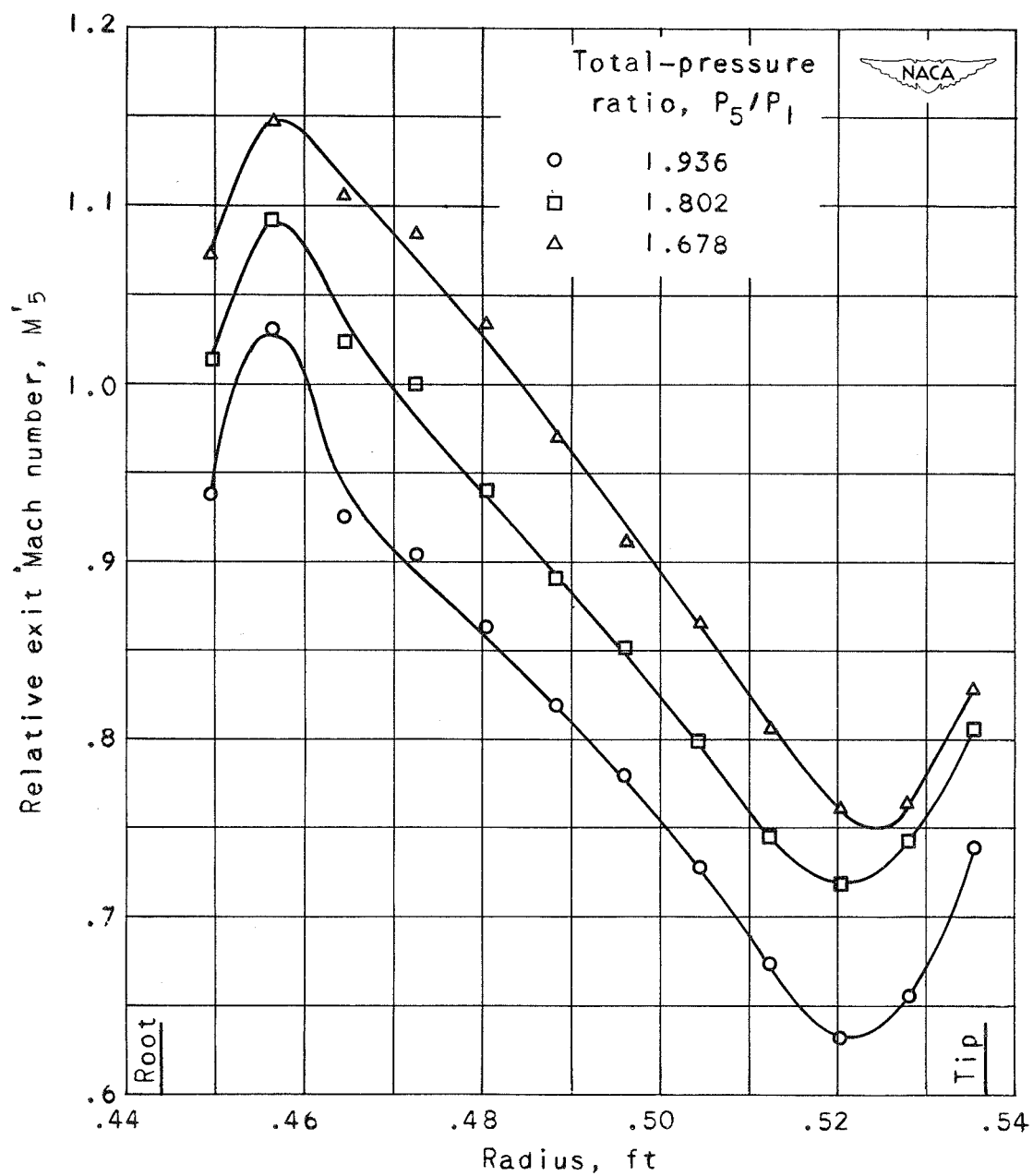radius at equivalent tip speed of 1396 feet per
second.

Figure 15. - Variation of relative exit Mach number
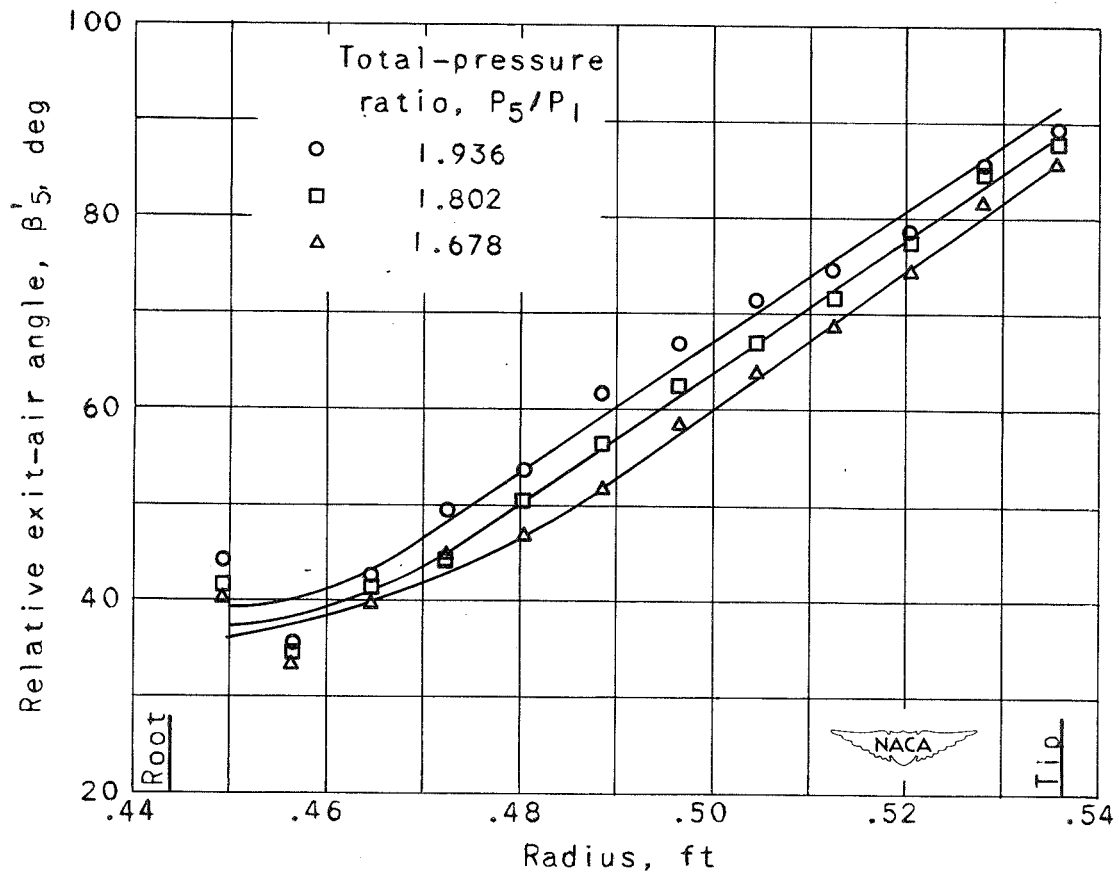with radius.

Figure 16. – Variation of relative exit-air angle
with radius at an equivalent tip speed of 1396
feet per second.

CONFIDENTIAL